

Supporting Information for

FruitFire: a luciferase based on a fruit fly metabolic enzyme

Spencer T. Adams, Jr., Jacqueto Zephyr, Markus F. Bohn, Celia Schiffer and Stephen C. Miller*

Department of Biochemistry and Molecular Biotechnology, UMass Chan Medical School, 364 Plantation St, Worcester, MA 01605

Stephen.miller@umassmed.edu

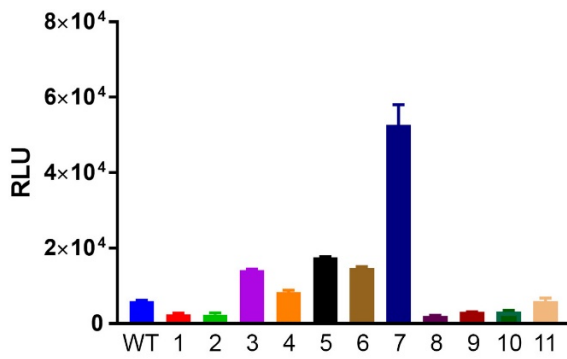
Table of Contents:

Supplementary Figures 1-6	S2-7
Supplementary Table 1	S8

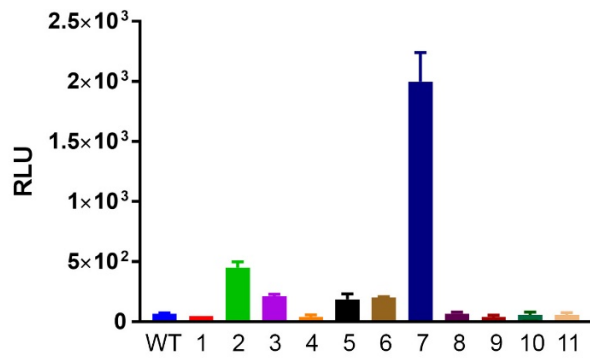
A

Mutant #	ASGG (312-315)	F → L (285)	TTSA (344-347)	LCGG (312-315)	TETTSA (342-347)	A → G (245)	T → R (219)
1	•	•					
2	•						
3	•		•				
4				•			
5					•	•	•
6					•	•	
7					•		
8	•	•			•	•	•
9	•	•			•	•	
10	•				•	•	•
11	•	•			•		•

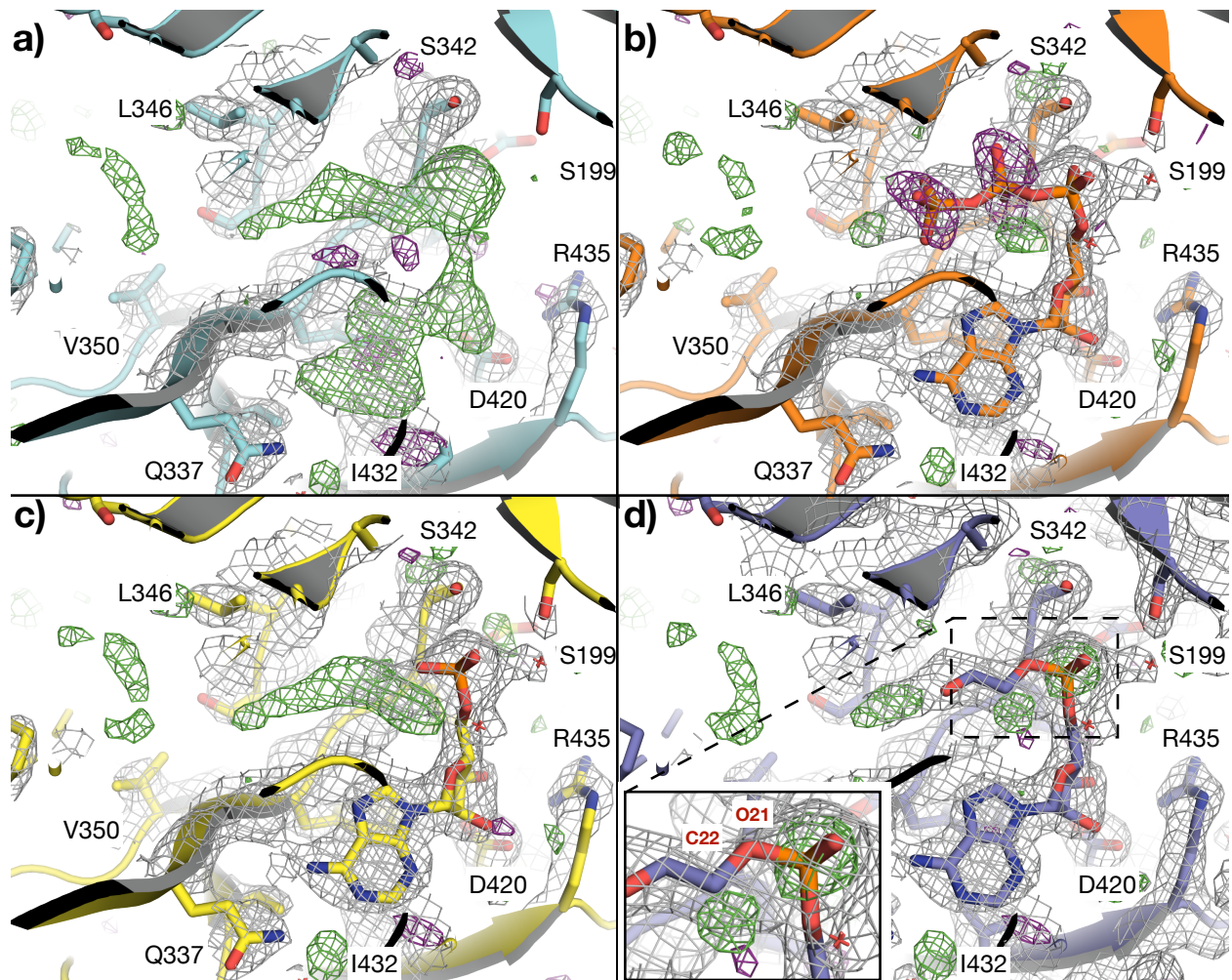
B



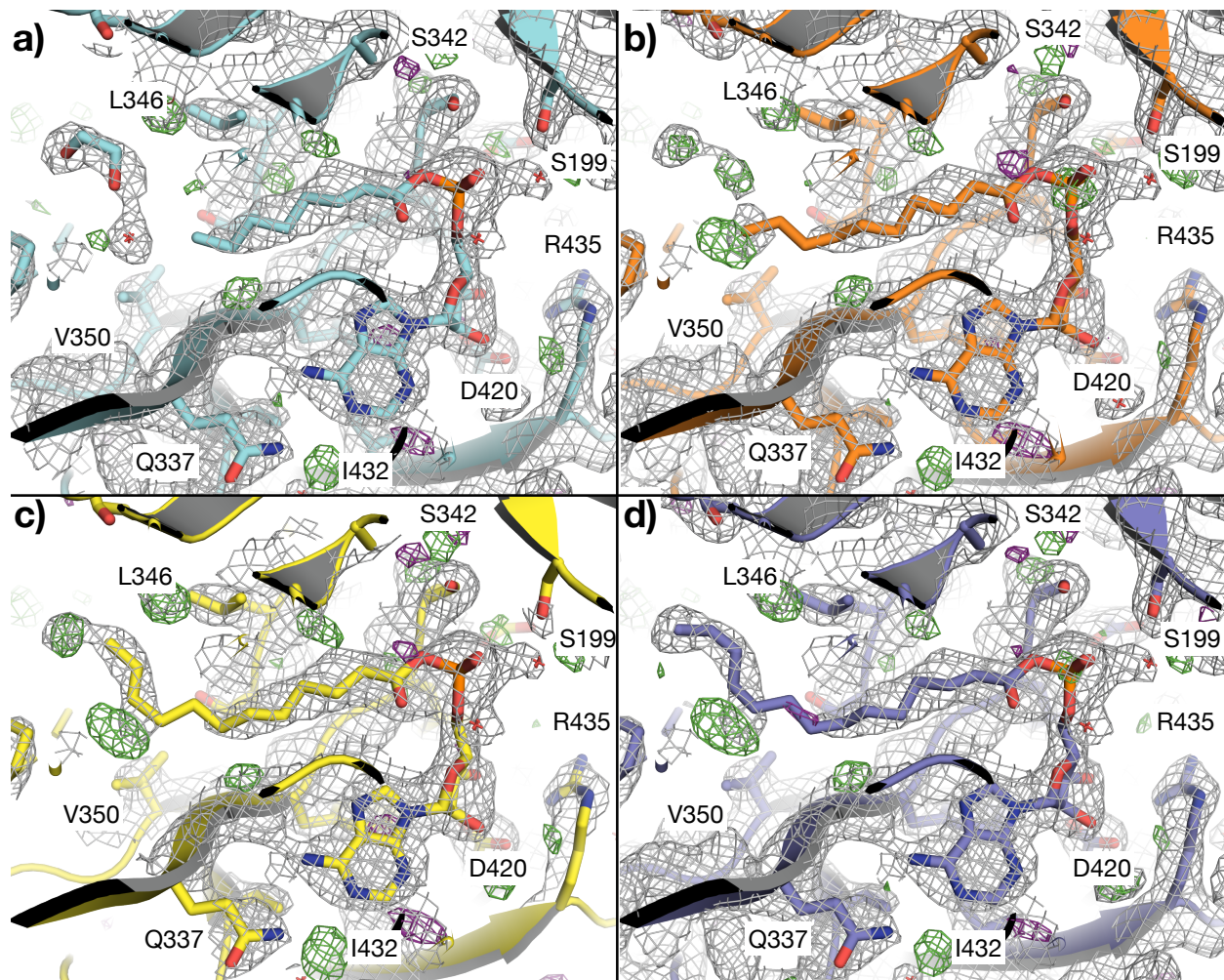
C



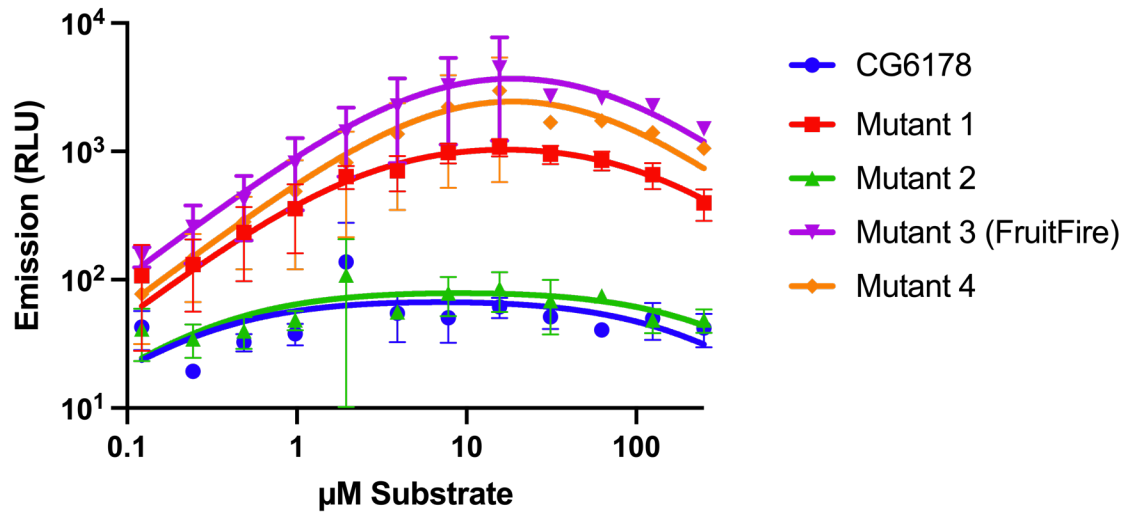
Supplementary Figure S1. *In vitro* activity of CG6178 active site mutants with CycLuc2 and D-luciferin. A) Residues in CG6178 highlighted in Figure 2 were replaced with the corresponding Fluc sequence in various combinations as shown. CG6178 and mutants 1-11 (40 nM) were mixed with 250 μ M of B) CycLuc2 or C) D-luciferin and light emission was measured with a Promega GloMax.



Supplementary Figure S2: ATP, AMP, and an adenylated ethylene glycol are insufficient to satisfy the density in the active site of CG6178. (a) The active site of CG6178 with no ligand modeled. (b) ATP, (c) AMP, and (d) an adenylated ethylene glycol molecule modeled in the ligand electron density. CG6178 is shown in cartoon representation. The 2Fo-Fc map (grey, at $\sigma = 1$) and Fo-Fc difference maps (green $\sigma = +3.0$ and purple $\sigma = -3.0$) are shown.

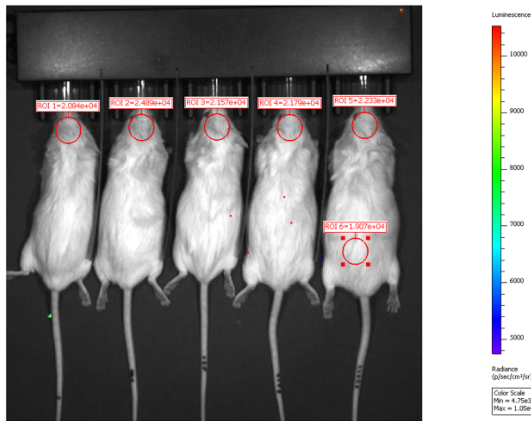


Supplementary Figure S3: Octanoyl-AMP (C8) represents the best model for the ligand density. (a) Octanoyl (C8), (b) Decanoyl (C10), (c) Dodecanoyl (C12), and (d) Myristoyl (C14) AMP esters modeled in the active site of CG6178. CG6178 is shown in cartoon representation. The 2Fo-Fc map (grey, at $\sigma = 1$) and Fo-Fc difference maps (green $\sigma = +3.0$ and purple $\sigma = -3.0$) are shown.

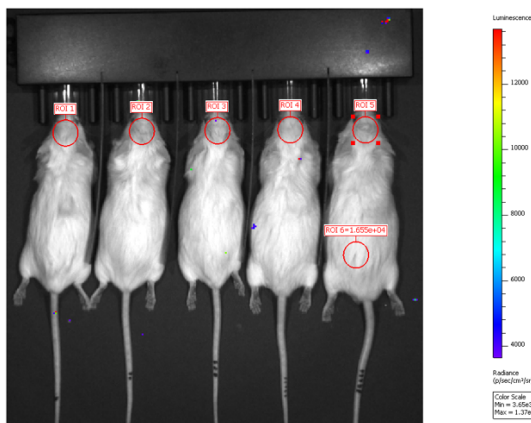


Supplementary Figure S4. *In vitro* performance of CG6178 and mutants with D-luciferin (0.122 - 250 μM). Signal from CG6178 and Mutant 2 is not above background.

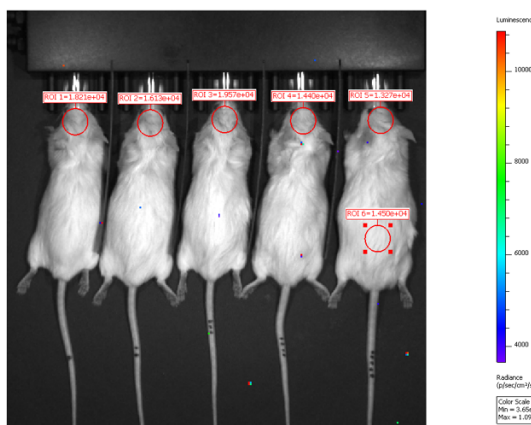
A



B

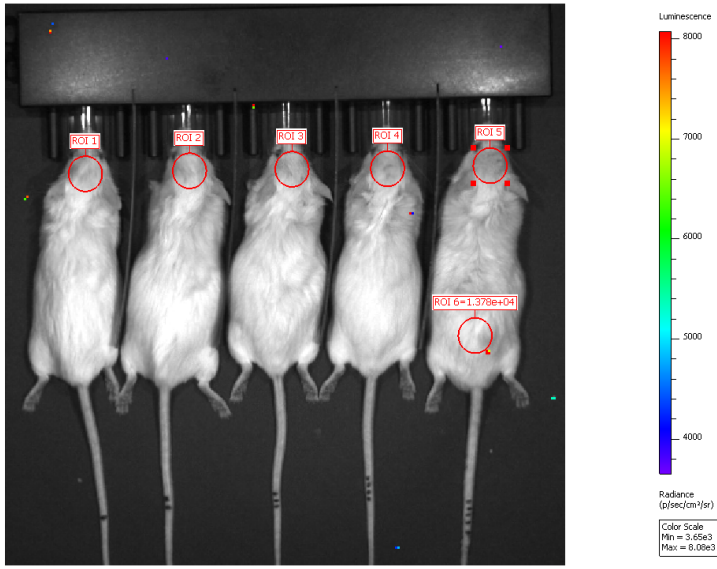


C

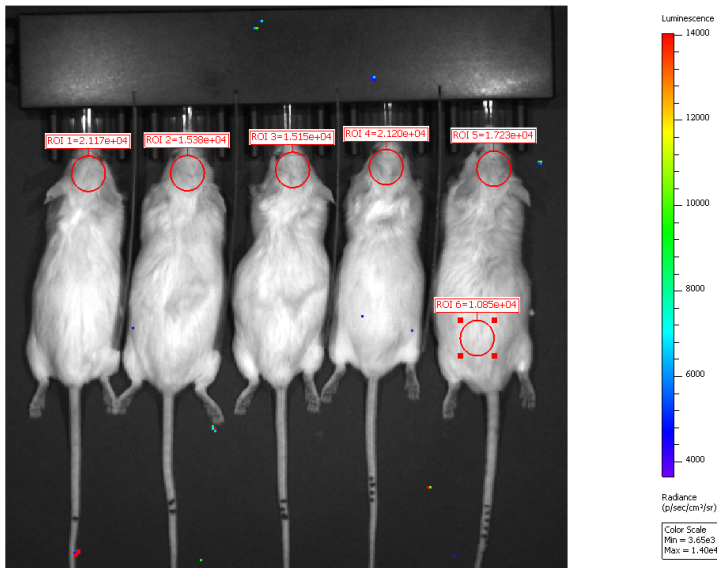


Supplementary Figure S5. Imaging of mice transduced in the striatum with CG6178. Mice were imaged after ip injection with A) 0.1 mL of 100 mM D-luciferin, B) 0.1 mL of 2.5 mM CycLuc2, or C) 0.1 mL of 250 μ M CycLuc2-amide.

A



B



Supplementary Figure S6. Imaging of mice transduced in the striatum with FruitFire. Mice were imaged after ip injection with A) 0.1 mL of 100 mM D-luciferin or B) 0.1 mL of 2.5 mM CycLuc2.

Table S1. Data collection and refinement statistics for CG6178.

Data Collection	
Wavelength	1.033
Resolution range	30.72 - 2.5 (2.589 - 2.5)
Space group	P 21 21 21
Unit cell	55.851 77.778 113.315 90 90 90
Total reflections	99870
Unique reflections	17673 (1726)
Multiplicity	5.6
Completeness (%)	99.80 (99.37)
Mean I/sigma(I)	17.46 (2.95)
Wilson B-factor	36.31
R-merge	0.104 (0.671)
Refinement	
Reflections used in refinement	17660 (1724)
Reflections used for R-free	885 (87)
R-work	0.1949 (0.2515)
R-free	0.2527 (0.3272)
Number of non-hydrogen atoms	4123
macromolecules	3988
ligands	69
solvent	99
Protein residues	534
RMS(bonds)	0.002
RMS(angles)	0.50
Ramachandran favored (%)	95.53
Ramachandran allowed (%)	4.72
Ramachandran outliers (%)	0.75
Rotamer outliers (%)	1.67
Clashscore	15.16
Average B-factor	38.72
macromolecules	38.72
ligands	42.50
solvent	37.28

Statistics for the highest-resolution shell are shown in parentheses.

^b R -merge = $\sum |I - \langle I \rangle| / \sum I$, where I = observed intensity, $\langle I \rangle$ = average intensity over symmetry equivalent; values in parentheses are for the highest resolution shell.

^cRMSD, root mean square deviation.

^d R -work = $\sum ||F_o| - |F_c|| / \sum |F_o|$.

^e R -free was calculated from 5% of reflections, chosen randomly, which were omitted from the refinement process